


RESEARCH

Open Access



Recombinant GH3 β -glucosidase stimulated by xylose and tolerant to furfural and 5-hydroxymethylfurfural obtained from *Aspergillus nidulans*

Diandra de Andrades^{1†}, Robson C. Alnoch^{1,2†}, Gabriela S. Alves^{2,3}, Jose C. S. Salgado^{1,4}, Paula Z. Almeida², Gabriela Leila Berto⁵, Fernando Segato⁵, Richard J. Ward⁴, Marcos S. Buckeridge⁶ and Maria de Lourdes T. M. Polizeli^{1,2*} 

Abstract

The β -glucosidase gene from *Aspergillus nidulans* FGSC A4 was cloned and overexpressed in the *A. nidulans* A773. The resulting purified β -glucosidase, named AnGH3, is a monomeric enzyme with a molecular weight of approximately 80 kDa, as confirmed by SDS-PAGE. Circular dichroism further validated its unique canonical barrel fold (β/α), a feature also observed in the 3D homology model of AnGH3. The most striking aspect of this recombinant enzyme is its robustness, as it retained 100% activity after 24 h of incubation at 45 and 50 °C and pH 6.0. Even at 55 °C, it maintained 72% of its enzymatic activity after 6 h of incubation at the same pH. The kinetic parameters V_{\max} , K_M , and K_{cat}/K_M for *p*-nitrophenyl- β -D-glucopyranoside (*p*NPG) and cellobiose were also determined. Using *p*NPG, the enzyme demonstrated a V_{\max} of 212 U mg⁻¹, K_M of 0.0607 mmol L⁻¹, and K_{cat}/K_M of 4521 mmol L⁻¹ s⁻¹ when incubated at pH 6.0 and 65 °C. The K_M , V_{\max} , and K_{cat}/K_M using cellobiose were 2.7 mmol L⁻¹, 57 U mg⁻¹, and 27 mmol⁻¹ s⁻¹, respectively. AnGH3 activity was significantly enhanced by xylose and ethanol at concentrations up to 1.5 mol L⁻¹ and 25%, respectively. Even in challenging conditions, at 65 °C and pH 6.0, the enzyme maintained its activity, retaining 100% and 70% of its initial activity in the presence of 200 mmol L⁻¹ furfural and 5-hydroxymethylfurfural (HMF), respectively. The potential of this enzyme was further demonstrated by its application in the saccharification of the forage grass *Panicum maximum*, where it led to a 48% increase in glucose release after 24 h. These unique characteristics, including high catalytic performance, good thermal stability in hydrolysis temperature, and tolerance to elevated concentrations of ethanol, D-xylose, furfural, and HMF, position this recombinant enzyme as a promising tool in the hydrolysis of lignocellulosic biomass as part of an efficient multi-enzyme cocktail, thereby opening new avenues in the field of biotechnology and enzymology.

Keywords Enzymatic hydrolysis, Xylose-stimulated, Tolerant to biomass products, Homologous expression

[†]Diandra de Andrades and Robson C. Alnoch contributed equally to this work.

*Correspondence:
Maria de Lourdes T. M. Polizeli
polizeli@ffclrp.usp.br

Full list of author information is available at the end of the article

Introduction

Lignocellulosic biomasses, abundant and renewable resources, have been identified as one of the most promising alternatives to meet increasing energy demands. Numerous studies have demonstrated the extensive potential of lignocellulosic biomass for the sustainable production of second-generation biofuels and various biomolecules and biomaterials with high-added value (McKendry 2002; Isikgor and Becer 2015; Mussatto et al. 2021; Alnoch et al. 2022). These biomasses primarily originate from plant cell walls and typically comprise 40–60% cellulose, 20–40% hemicellulose, and 10–25% aromatic hydrocarbon lignin (Zoghlami and Paës 2019; Srivastava et al. 2019).

Cellulose, a long-chain homopolymer comprising D-anhydroglucopyranose units covalently linked by β -(1,4) glycosidic bonds, exhibits a high degree of polymerization (DP) and molecular weight (Brigham 2018; Acharya et al. 2021). Due to its polysaccharide structure, cellulose contains numerous hydroxyl groups in the D-glucose units. It forms robust intra- and intermolecular hydrogen bond networks, resulting in a compact crystalline structure (highly ordered region) (Alves et al. 2018; Zoghlami and Paës 2019; Michelin et al. 2020; Etale et al. 2023). Moreover, partial cellulose chains are irregularly arranged, constituting the amorphous region of cellulose (the disordered region). Thus, although cellulose ranks among the most recalcitrant materials, it is also one of the most abundant biomaterials on Earth, harboring significant biotechnological potential (Sun et al. 2016; Alves et al. 2018; Zoghlami and Paës 2019; Michelin et al. 2020).

The complete enzymatic conversion of the cellulose into monomeric sugars requires synergistic interactions among the cellulolytic complex enzymes, including endoglucanases, cellobiohydrolases, and β -glucosidases. Endo-1,4- β -glucanases (EC 3.2.1.4) hydrolyze the β -1,4 glycosidic bonds randomly within the amorphous cellulose structure, releasing oligosaccharides of varying DPs. Cellobiohydrolases (CBH, exo-1,4- β -glucanases, EC 3.2.1.91 and 3.2.1.176) cleave the ends of cellulose chains (both reduced and non-reduced), releasing oligosaccharides, primarily cellobiose units (Bajpai 2018; Hildén and Mäkelä 2018; Srivastava et al. 2019).

The third enzyme group in the complex comprises β -glucosidases (β -D-glucopyranoside glucohydrolase; EC 3.2.1.21), crucial for hydrolyzing β -1,4-glycosidic bond in oligosaccharides, aryl-, and alkyl β -glucosides, as well as disaccharides, releasing the glucose monomer (Chang et al. 2018; Salgado et al. 2018). Other essential enzymes include lytic polysaccharide monoxygenases (LPMOs, AA9 to 11 and AA12 to 17, EC 1.14.99.54 and EC 1.14.99.56), which utilize a copper-dependent oxidative mechanism to break cellulose chains, and

carbohydrate-specific oxidoreductases such as cellobiose dehydrogenase (CDH, AA3, EC 1.1.99.18) and cellooligosaccharide dehydrogenase (AA7, EC 1.1.99.-), which donate electrons to LPMOs during the carbohydrate oxidation process (Freitas et al. 2021b; Alnoch et al. 2023).

The β -glucosidases have been extensively studied for their broad applications in food, feed, textile, and paper industries (de Andrades et al. 2019a; Mishra et al. 2019). They are critical enzymes in biorefineries, facilitating the release of sugar monomers through enzymatic saccharification of cellulose. By hydrolyzing oligosaccharides and cellobiose (which are potent inhibitors of the activities of most cellobiohydrolases and endoglucanases), β -glucosidases play a crucial role (Singhania et al. 2011; Fusco et al. 2018; Huang et al. 2021). Moreover, the synergism between cellulolytic complex enzymes is essential for biomass degradation, as it can accelerate and increase hydrolysis yield (Agrawal et al. 2018; Alves et al. 2018).

Compounds released during pretreatment of lignocellulosic biomass, such as furfural or hydroxymethylfurfural (HMF), may inhibit these enzymes or disrupt their synergistic effects. Consequently, there is an increasing demand for biocatalysts with improved properties for industrial applications, such as increased stability at high temperatures and wide pH range and tolerance to toxic compounds resulting from the process (Wojtusik et al. 2017; Alves et al. 2018).

Filamentous fungi are widely employed as hosts for protein production in various biotechnological applications. The main advantage of using microbial systems lies in their rapid growth on cost-effective substrates, along with well-known genetics and physiology (Kück and Hoff 2010; Ward 2012; Daly et al. 2017; Yan et al. 2023). *Aspergillus nidulans* is among the foremost laboratory model systems for protein cell-factory since it has a protein synthesis machinery well that can produce and secrete amounts of proteins (Lubertozzi and Keasling 2009; Fleissner and Dersch 2010; Segato et al. 2012). For instance, several CAZymes have been successfully overexpressed in the last few years using a high expression pEXPYR vector integrated into *A. nidulans* A773 host (Segato et al. 2012; Ribeiro et al. 2014; Velasco et al. 2020; Liu et al. 2021; Gonçalves et al. 2023; Alnoch et al. 2023). In brief, the pEXPYR vector contains the glucoamylase promoter (*glaAp*) and secretion peptide (*glaAsp*) of *Aspergillus niger*, which enables the maltose-induced expression, high-yield secretion and accumulation of the recombinant enzyme in the extracellular medium (Segato et al. 2012).

Considering all these aspects, this work aimed to report the cloning, production, purification, kinetics, and biochemical characterization of a β -glucosidase (GH3) expressed in homologous host *A. nidulans* A773. For this, the thermal and pH stabilities, the specificity on different

substrates, and its tolerance to compounds commonly found in the reaction medium for the hydrolysis of lignocellulosic residues and high added value compounds production, such as glucose, xylose, ethanol, furfural, and HMF were evaluated. Additionally, the potential application of AnGH3 in the hydrolysis of cellulosic biomass using forage grass *P. maximum* was also analyzed.

Materials and methods

Reagents and suppliers

The following substrates ρ -nitrophenyl- β -D-glucopyranoside (ρ NPG), ρ -nitrophenyl- β -D-galactopyranoside (ρ NPGal), ρ -nitrophenyl- α -D-glucopyranoside (α - ρ NPG), ρ -nitrophenyl- β -D-cellobioside (ρ NPCel), ρ -nitrophenyl- β -D-xylopyranoside (ρ NPX), cellobiose, salicin, carboxymethylcellulose (CMC) and reagents 3,5-dinitrosalicylic acid (DNS), furfural (99%) and 5-(hydroxymethyl)furfural (99%) were purchased from Sigma-Aldrich (St. Louis, USA). Precision Plus Protein Dual Color Standards and Bradford Protein assay were obtained from Bio-Rad Laboratories (Hercules, CA, USA). All other reagents used were of analytical grade.

Cloning, transformation, and screening of recombinant transformants

A. nidulans strains FGSC A4 and A773 (*pyrG89*; *wA3*; *pyroA4*) were obtained from the Fungal Genetics collection (FGSC, Kansas City, MO, USA). Genomic DNA extraction from *A. nidulans* FGSC A4 was carried out using the Wizard Genomic DNA Purification Kit (Promega, Madison, WI, USA). The oligonucleotides AnGH3F (forward, 5'-CATTACACCTCAGCAATGC GCTCTCTGATAAGATCCGGCG-3'; and AnGH3R (reverse, 5'-GTCCCGTGCCGGTTACTAGACGGTA AAGCTTCCCGTCAACCG-3') were designed based on the GH3 coding sequence *angh3* (access number XM_655340.1) and amplified from genomic DNA by PCR and then cloned into the pEXPYR expression vector using the Gibson Assembly method (Gibson et al. 2009). The resulting construct, pEXPYR-*angh3*, was transformed into the *A. nidulans* A773. Minimal media without uracil and uridine was used to select positive clones (Segato et al. 2012). SDS-PAGE confirmed the expression of AnGH3 by recombinant strains.

Expression and purification of recombinant AnGH3

The culture medium consisted of 10 g of glucose, pyridoxine (1 mg L⁻¹), 50 mL of Clutterbuck salts (30.4 g KH₂PO₄, 120 g NaNO₃, 10.4 g MgSO₄·7H₂O and 10.4 g KCl, per liter), 1 mL of trace elements (5 g Na₂EDTA, 2.2 g ZnSO₄·7H₂O, 0.11 g Na₂MoO₄·4H₂O, 0.5 g MnCl₂·4H₂O, 0.5 g FeSO₄·7H₂O, 0.16 g CuSO₄·5H₂O,

0.16 g CoCl₂·5H₂O, and 1.1 g H₃BO₃ in 100 ml), pH 6.5 (Segato et al. 2012).

The crude extract obtained was filtered through a Büchner funnel with Whatman n°1 filter paper, concentrated by ultrafiltration, and equilibrated using a 10 kDa cut-off membrane (Hollow Fiber Cartridge GE Healthcare) coupled in QuixStand Benchtop Systems. Subsequently, the purification process was performed using an ÄKTA Purifier system (GE Healthcare). The crude extract was loaded into an anion exchange Hiprep Q FF column (GE Healthcare) previously equilibrated in 50 mmol L⁻¹ phosphate buffer, pH 6.5, with a flow rate of 1 mL min⁻¹. Protein levels were monitored at 280 nm and eluted with a linear gradient from 0 to 1 mol L⁻¹ of NaCl (Alnoch et al. 2023). The recovered sample was then applied to a size exclusion chromatography (Superdex 75 10/300 GL GE Healthcare) column equilibrated in 50 mmol L⁻¹ phosphate buffer and 150 mmol L⁻¹ NaCl, pH 6.5, at a flow rate of 0.5 mL min⁻¹. Protein fractions exhibiting the highest β -glucosidase activities were selected via SDS-PAGE electrophoresis, pooled, ultrafiltered, and dialyzed using a 10 kDa cut-off membrane.

Enzymatic assays

The β -glucosidase activity was quantified using ρ NPG or cellobiose as substrate. The ρ NPG assays utilized 50 μ L of ρ NPG 4 mmol L⁻¹, 30 μ L of phosphate buffer 100 mmol L⁻¹ at pH 6.0, and 20 μ L of enzyme solution (4 μ g). The assay was carried out at 65 °C for 2 min, stopped with 100 μ L of 0.5 mol L⁻¹ Na₂CO₃ (pH 10). The released ρ -nitrophenolate was quantified at 410 nm using ρ -nitrophenol as a standard in the calibration curve.

Activity assays with cellobiose were performed using 50 μ L of 25 mmol L⁻¹ cellobiose, 30 μ L of 100 mmol L⁻¹ phosphate buffer at pH 6.0, and 20 μ L of enzyme solution. The assay was carried out at 65 °C for 5 min, stopped by boiling for 5 min, followed by cooling in an ice bath. The amount of released glucose was measured using a glucose oxidase enzymatic assay kit (glucose liquiform, Labtest, Brazil). A volume of 10 μ L of the previous mixture assay and 1 mL of the reagent solution kit were incubated at 37 °C for 10 min, and the absorbance was measured at 505 nm, with glucose used as standard in the calibration curve.

For both assays, one unit of enzyme activity (U) was defined as the amount of enzyme that catalyzes the release of 1 μ mol of ρ -nitrophenolate or glucose per minute under assay conditions.

Protein determination and electrophoresis analysis

The Bradford method was used to determine protein content (Bradford 1976), with bovine serum albumin as the standard. Electrophoresis of the protein samples (12% SDS-PAGE) was performed according to Laemmli

(Laemmli 1970), using a molecular standard of 10 to 250 kDa (Precision Plus Protein™ Standards Bio–Rad). The gel was stained with Coomassie brilliant blue 0.05% (m v^{-1}).

Circular dichroism analysis

Circular dichroism analysis (CD) was performed in a Jasco-810 spectropolarimeter (JASCO Inc., Tokyo, Japan), as previously described (Alnoch et al. 2023). Protein samples ($0.1\text{--}1\text{ mg mL}^{-1}$) were mixed in 10 mmol L^{-1} Tris–HCl buffer pH 7.0 and added in a quartz cuvette of $200\text{ }\mu\text{L}$, with an optical path length of 0.1 mm . Data were collected at a scanning speed of 50 nm min^{-1} , a spectral bandwidth of 3 nm , and a response time of 1 s . Blank spectra with the buffer only were subtracted in all experiments. Measurements comprised six accumulations within the UV range UV of $190\text{--}250\text{ nm}$. Analyses of the CD spectral data were performed with the DichroWeb server (Miles et al. 2022).

Matrix-assisted laser desorption ionization-time of flight mass spectrometry (MALDI-TOF MS) analysis

For this procedure, $100\text{ }\mu\text{g}$ of purified AnGH3 (lyophilized) was resuspended in a solution containing 8.0 mol L^{-1} urea ($\text{CH}_4\text{N}_2\text{O}$), 100 mmol L^{-1} Tris–HCl, pH 8.5. Subsequently, the samples were treated with $100\text{ }\mu\text{g}$ of dithiothreitol (DTT) at $37\text{ }^\circ\text{C}$ for 60 min , followed by alkylation with $300\text{ }\mu\text{g}$ of iodoacetamide at $37\text{ }^\circ\text{C}$ for 60 min before tryptic digestion at $37\text{ }^\circ\text{C}$ overnight. The mass spectra were obtained using a MALDI–TOF–TOF/MS (AutoFlex Max, Bruker). The obtained mass profiles were compared with peptide masses predicted through in silico digestion using the MS-Digest tool in Protein Prospector (Perkins et al. 1999) and MASCOT server (Chalkley et al. 2005).

Sequence analysis and structural homology modeling

Sequence alignment was carried out using MEGA software version 11.0, employing the ClustalW algorithm (Thompson et al. 1994). Protein sequences were retrieved from the Protein Data Bank (PDB) (Berman et al. 2000). The ENDscript server (Robert and Gouet 2014) was utilized to predict the secondary structure and features of the amino acid sequence based on PDB templates. Homology modeling of AnGH3 was performed using AlphaFold2 (Jumper et al. 2021), integrated into UCSF ChimeraX (Pettersen et al. 2021).

Deglycosylation analysis

The deglycosylation (*N*-glycosylation) assay was carried out using Endoglycosidase H (EndoH) (Roche, Mannheim, DE). For this assay, $5\text{ }\mu\text{g}$ of purified AnGH3 was mixed with 250 mU of EndoH in a sodium acetate buffer (50 mmol L^{-1} , pH 5.5) and maintained at $37\text{ }^\circ\text{C}$ for

16 h . The samples were then analyzed using SDS–PAGE, and the samples were compared before and after treatment. To estimate the carbohydrate content, we compared the migration difference between the treated and untreated samples with that of the molecular mass standard (Wilson et al. 2009; Alnoch et al. 2023).

Biochemical characterization of the AnGH3

Effect of temperature and pH on AnGH3 activity and stability

The effect of temperature on AnGH3 activity was assessed by measuring the hydrolysis of cellobiose across a temperature range of $35\text{ to }85\text{ }^\circ\text{C}$, utilizing 50 mmol L^{-1} sodium phosphate buffer at pH 6.0. AnGH3 was incubated for 24 h at $45\text{ to }60\text{ }^\circ\text{C}$ to evaluate the thermal stability.

The influence of pH on AnGH3 activity was investigated at $50\text{ }^\circ\text{C}$, over the range of $3.0\text{ to }9.0$, using: pH $3.0\text{--}5.5$ (50 mmol L^{-1} sodium citrate buffer), pH $5.5\text{--}7.5$ (50 mmol L^{-1} sodium phosphate buffer), and pH $7.5\text{--}9.0$ (50 mmol L^{-1} Tris–HCl buffer). The enzyme was incubated for 24 h at $25\text{ }^\circ\text{C}$ across a pH range of $3.0\text{ to }9.0$ for pH stability determination. Residual activity was calculated relative to the initial enzyme activity.

Substrate specificity

To determine the substrate specificity of the enzyme, ρNPG , ρNPGal , ρNPX , $\alpha\text{-}\rho\text{NPG}$, ρNPCel , CMC, cellobiose, lactose, and salicin, were utilized as substrates to evaluate the enzymatic activity in 100 mmol L^{-1} phosphate buffer, pH 6.5, at $65\text{ }^\circ\text{C}$. For ρNP substrates, the reactions were monitored by the ρNP -releasing assay described above. Glucose release from cellobiose, lactose, and salicin was determined using the glucose oxidase-based kit, while reducing sugar release from other substrates was determined using the DNS method (Miller 1959).

Effect of different compounds on AnGH3 activity

The impact of various concentrations of xylose ($0\text{--}2\text{ mol L}^{-1}$), glucose ($0\text{--}1\text{ mol L}^{-1}$), furfural ($0\text{--}200\text{ mmol L}^{-1}$), 5–HMF ($0\text{--}200\text{ mmol L}^{-1}$), and ethanol ($1\text{--}50\%\text{ v/v}$), on AnGH3 activity were assessed by incubating the purified enzyme as described in Sect. 2.4. The residual activity was determined by comparing enzyme activity at each additive concentration to the control without additives.

Determination of kinetic parameters

The Michaelis-Menten constant (K_M) and maximum velocity (V_{max}) of AnGH3 (0.2 mg mL^{-1}) were determined using ρNPG and cellobiose as substrates, with concentrations varying from $0.004\text{ to }4\text{ mmol L}^{-1}$ and $2\text{ to }20\text{ mmol L}^{-1}$, respectively. Assays were conducted at pH 6.0 and $65\text{ }^\circ\text{C}$, and the parameters were calculated using the Hanes method (Hanes 1932) with GraphPad

Prism 8.0 software (GraphPad Software, LLC). Turnover number (k_{cat}) and catalytic efficiency (K_{cat}/K_M) were also calculated.

Enzymatic saccharification of biomass

To assess the potential application of AnGH3 in the hydrolysis of cellulosic biomass, the conversion of tropical forage grass (*Panicum maximum*) using the commercial preparation Celluclast® 1.5 L (with or without AnGH3) was performed. The enzymatic conversion process was carried out using a substrate concentration of 3% (w/v, dry basis) in 50 mmol L⁻¹ citrate buffer pH 5.0. The commercial Celluclast® 1.5 L (Novozymes, Denmark) load was 20 filter paper units (FPU) per gram of biomass, while the purified enzyme was loaded at 69 U per gram of biomass. The assay mixture was incubated in a Thermomixer C (Eppendorf, Hamburg, Germany) for 24 h at 50 °C and 1300 rpm. Following hydrolysis, the total glucose released was quantified using the glucose oxidase

method (Labtest, Brazil), with glucose as the standard (de Andrades et al 2019b). A control experiment was performed by hydrolysis of biomass without adding the enzyme to the reaction medium.

Results and discussion

Sequence analysis and molecular modeling

The β-glucosidase AnGH3 from *A. nidulans* comprises 718 amino acid residues, including a 19 residues signal peptide, with the N-terminus in mature protein initiating with residues TGQVL (Fig. 1). To elucidate the characteristics of AnGH3 concerning the GH3 β-glucosidase utilized as a template for the 3D model, multiple sequence-structure alignments were conducted between the β-glucosidases from *Chaetomella raphigera* [PDB: 6JXG], and *Hypocrea jecorina* [PDB: 3ZYZ] (Fig. 2A). The 3D model and structure alignment revealed the distinctive structure of the β-glucosidase GH3, featuring a three domains structure, within domain I between the residues

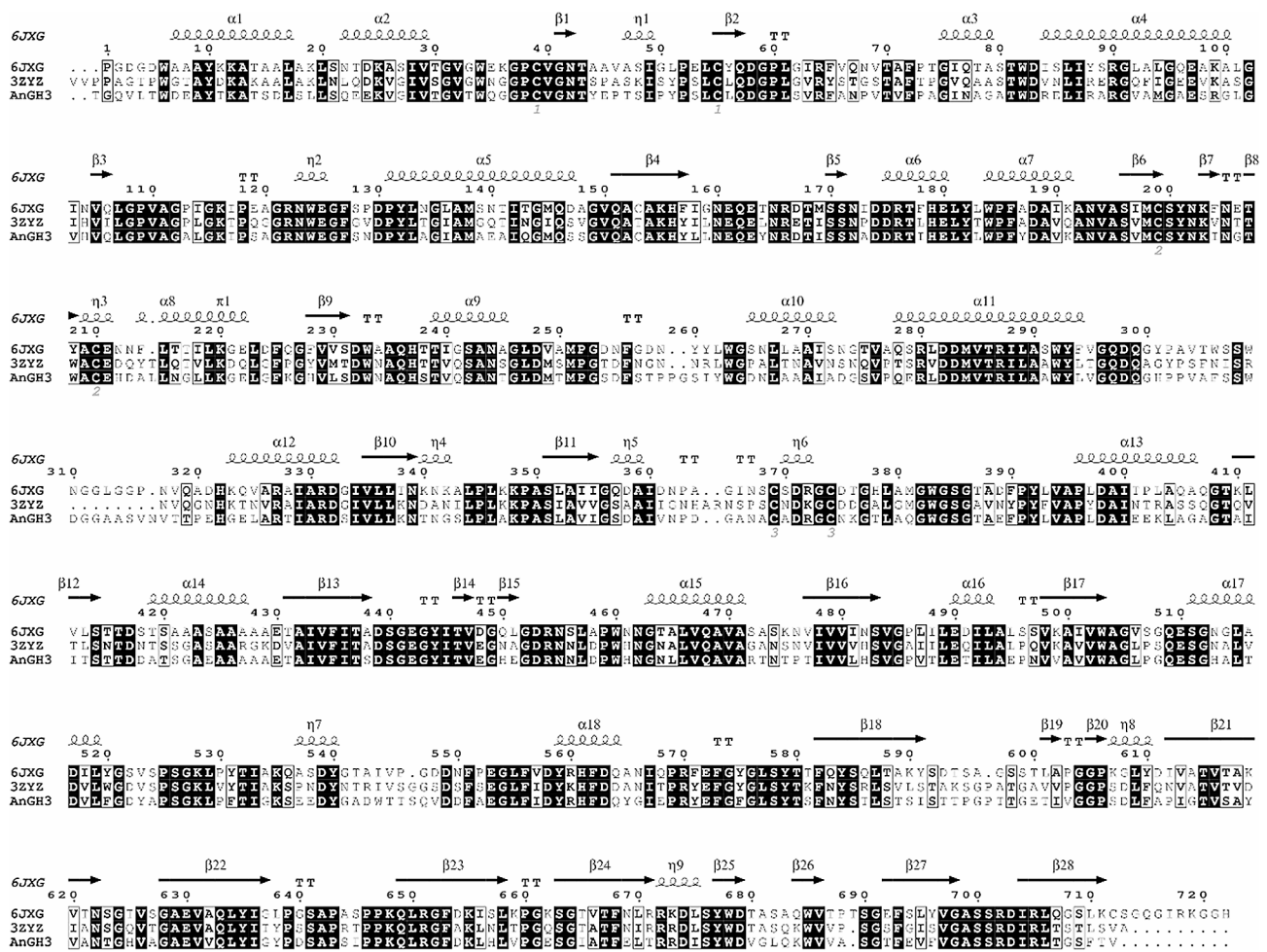


Fig. 1 Multiple sequence alignment and secondary structure prediction of AnGH3 and PDB template. Access codes: *C. raphigera* [PDB: 6JXG] and *H. jecorina* [PDB: 3ZYZ]. Dark- and light-shaded boxes indicate conserved residues. Secondary structures representations: arrows represent β-strands, α-helices are represented by α, and β-turns are marked with TT. Sequence alignments were performed using Clustal (Thompson et al. 1994), and the figure was prepared using ESPriptS.

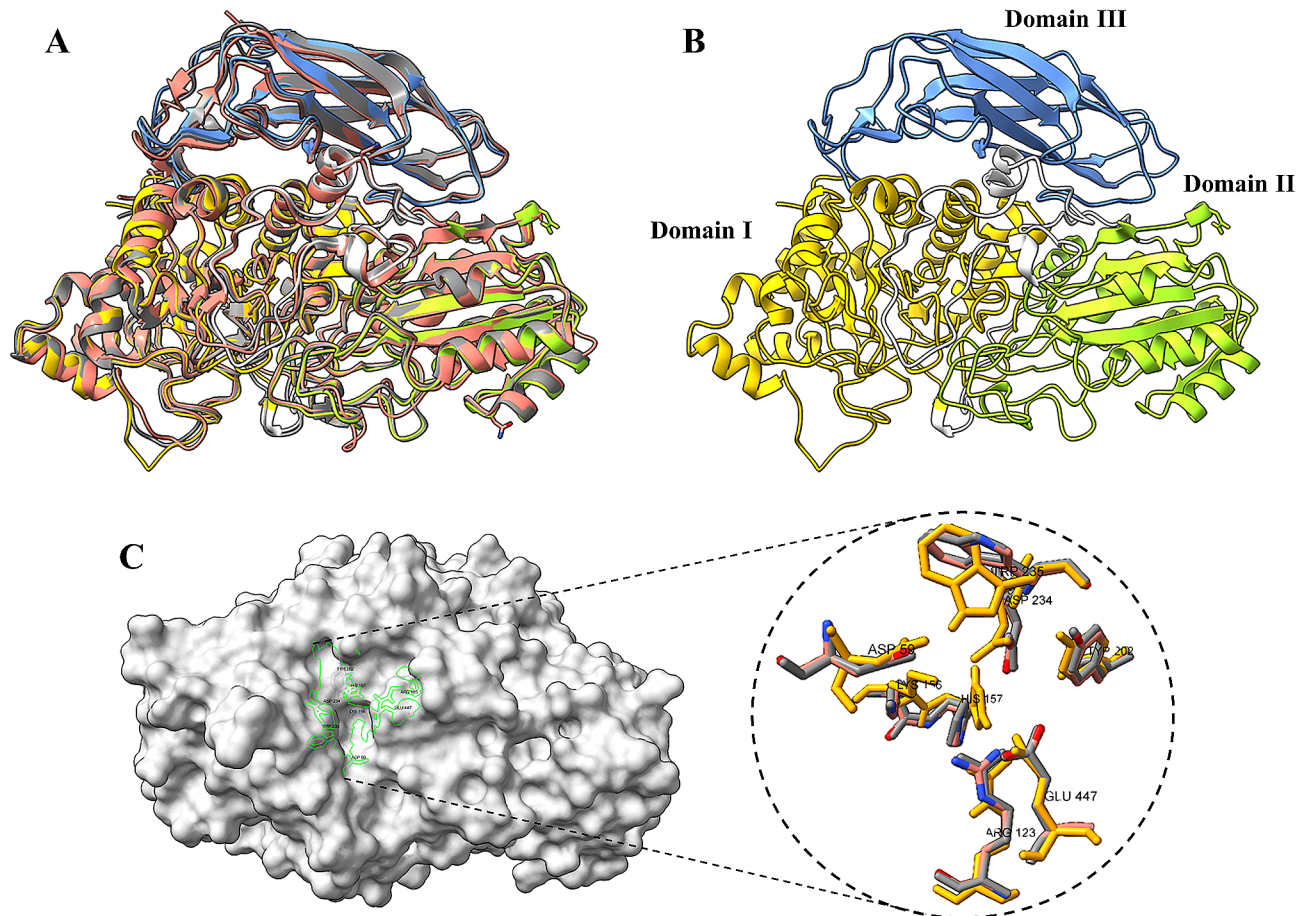


Fig. 2 Schematic representation of the overall structure of AnGH3. **(A)** 3D model of AnGH3 superimposed with template structures from *C. raphigera* [PDB: 6JXG] (gray) and *H. jecorina* [PDB: 3ZYZ] (magenta). **(B)** 3D model of AnGH3 with the three domains are colored yellow (domain I), green (domain II), and blue (domain III). The two domain linker regions are shown in white. **(C)** Zoom-in of the modeled catalytic tunnel. The Figure was prepared using UCSF ChimeraX

1 to 312; domain II presenting a structural characteristic of α/β sandwich between residues 325 to 526 and the domain III composed of residues 578 to 718 with an immunoglobulin-like topology (Fig. 2B).

Alignment of the structure and 3D model facilitated the identification of essential amino acid residues within the active site of AnGH3, aligning with analogous in other GH3 β -glucosidase (Karkehabadi et al. 2014; Kao et al. 2019). Asp²³⁴ and Glu⁴⁴⁷ serve as nucleophilic and acid/base residues, corresponding to Asp²³² and Glu⁴⁴² in the model PDB: 6JXG and Asp²³⁶ and Glu⁴⁴¹ in the model PDB: 3ZYZ, indicating their consistent catalytic site function (Fig. 2C). Residues Asp⁵⁹, Arg¹²³, Lys¹⁵⁶, His¹⁵⁷, and Trp²³⁵ constitute a substrate binding subsite, mirroring the crystal structures of *C. raphigera* and *H. jecorina* β -glucosidases in the same positions. However, Trp²³⁵ exhibits a distinct orientation compared to Trp²³³ in the structure PDB: 6JXG and Trp²³⁷ in PDB: 3ZYZ (Fig. 2C). The observed molecular weight variation (77.6 to 80.2 kDa) suggests glycosylation sites in AnGH3

(Fig. 3A). Three N-glycosylation sites (N²⁰⁶, N³²¹ and N³⁴⁶) were predicted within the AnGH3 sequence using NetNGlyc – 1.0 Server (Gupta and Brunak 2002).

Purification and identification AnGH3

Recombinant AnGH3 was successfully expressed in *A. nidulans* strain A773 and purified. AnGH3 is a monomeric enzyme, and the homogeneity of the purified AnGH3 was evidenced as a single band in SDS-PAGE (Fig. 3A), exhibiting an apparent molecular weight of approximately 80.2 kDa. Mass spectrometry confirmed that the band in the SDS-PAGE corresponds to the recombinant AnGH3 (Fig. S1).

Endo H was used for enzymatic deglycosylation assay. The profiles of native AnGH3 (80.2 kDa) and deglycosylated AnGH3 can be distinguished in lanes 1–2 (Fig. 3A). Deglycosylated AnGH3 exhibited an estimated molecular weight of 77.6 kDa, consistent with the theoretical molecular weight of 75.9 kDa for the AnGH3 sequence. Consequently, the results suggest a carbohydrate content

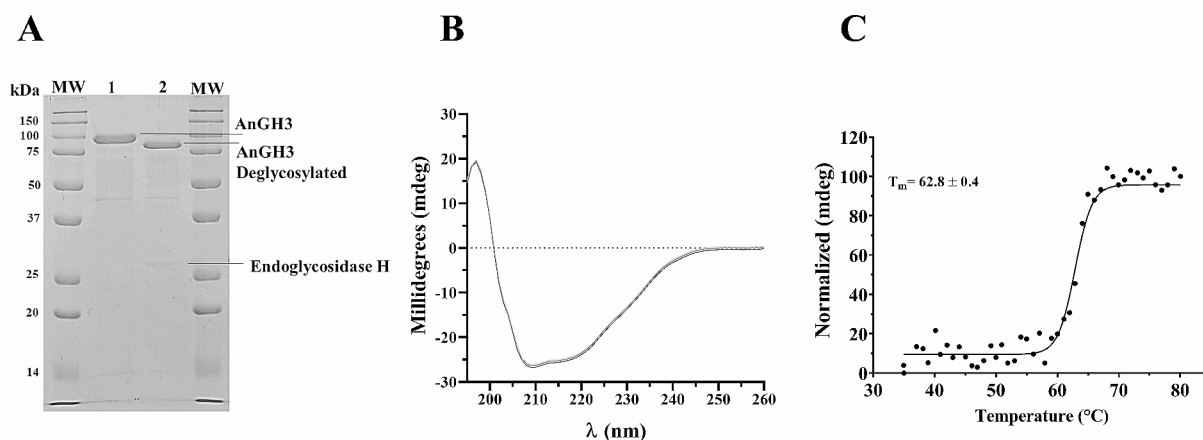


Fig. 3 (A) Purification of the recombinant β -glucosidase AnGH3 from *A. nidulans*. SDS-PAGE of AnGH3 (line 1) from size exclusion Superdex 75 10/300 GL column and (lane 2) analysis of the enzymatic deglycosylation assay after digestion treatment with endoglycosidase H. MW: molecular weight standard ladder. (B) The secondary structure profile of purified AnGH3 was determined by CD spectroscopy. (C). Thermal stability curve of AnGH3 determination of melting temperature (T_m)

of approximately 4% of the molecular weight of native AnGH3.

Circular dichroism spectra of AnGH3 revealed a negative band at 208 and 222 nm, characteristic of α -helix structure, and an upbeat band at 218 nm corresponding to β -sheets (Fig. 3B), matching content of α -helix, β -sheets and a random coil of 38%, 26% and 37%, respectively. These features align with the canonical barrel fold (β/α), as also observed in the 3D homology model of AnGH3. Figure 3C illustrates that the melting temperature (T_m) of the enzyme was 62.8 °C at pH 7.0. Similar results regarding the impact of temperature on secondary structure were reported for other GH3 enzymes (Méndez-Líter et al. 2017; Lima et al. 2020).

The specific activity of AnGH3 was determined to be $282 \pm 17 \text{ U mg}^{-1}$, utilizing ρ NPG as substrate, at pH 6.0, 65 °C. This preparation was used for biochemical characterization assays.

Biochemical characterization assays

Effect of pH and temperature on activity and stability of AnGH3

The effects of pH and temperature on the activity and stability of the AnGH3 were also analyzed. Figure 4A demonstrates that AnGH3 exhibits activity over a broad range of pH values (4.5–9.0), with a maximum at pH 6.0 (55.4 U mg^{-1}). At pH 7.5, the activity decreased to 67% or even to 48%, depending on the used buffer, indicating a significant influence of the buffer on AnGH3 activity, with sodium phosphate buffer providing more effective than Tris–HCl (Fig. 4A). AnGH3 remained fully active across a wide pH range (4.5 to 9.0), showing 100% of residual activity after 24 h of incubation (Fig. 4C). Additionally, AnGH3 retained 70 and 93% of its activity after 24 h of

incubation at pH 3.5 and 4.0, respectively (Fig. 4C). These optimal pH conditions align with those described for recombinant enzymes such as BgL1 from *A. niger* BE-2 (Ali et al. 2016) and TrBgl2 from *Trichoderma reesei* (Solhtalab et al. 2019), confirming the reported optimal pH values between 4.0 and 6.0 for fungal β -glucosidases (Bonfá et al. 2018).

The optimal temperature for maximal AnGH3 activity was achieved around 65 and 70 °C, at pH 6.0 (56 U mg^{-1}) (Fig. 4B). The soluble enzyme remained completely stable at 45 and 50 °C after 24 h of the incubation (Fig. 4D). However, after 6 h of incubation at 55 °C, its enzymatic activity was reduced to 72%. Similar properties have been reported for other recombinant β -glucosidases expressed in *Pichia pastoris*. For instance, MtBgl3b from *Myceliophthora thermophila* exhibited maximum activity at 60 °C and pH 5.0, retaining about 90% of its relative activity at 60 °C for 120 min (Zhao et al. 2015). A BGL2 from *Neurospora crassa* displayed its highest activity at pH 5.4 and 60 °C, retaining 88.1 and 62.6% of its relative activity at 50 and 55 °C, respectively, after 20 min (Pei et al. 2016). The Bgl4 from *Penicillium funiculosum* NCL1 showed optimal activity at pH 5.0 and 60 °C, retaining 77% of its initial activity after 1 h of incubation at 60 °C (Ramani et al. 2015). These thermostable enzymes offer advantages in processes at higher temperatures, mainly concerning better substrate solubility and mass transfer (Turner et al. 2007; Sharma et al. 2019). Aiming to broaden the use of β -glucosidases in industry, it would be beneficial to use enzymes that tolerate non-mild conditions such as high temperatures and extreme pH values (Ouyang et al. 2023).

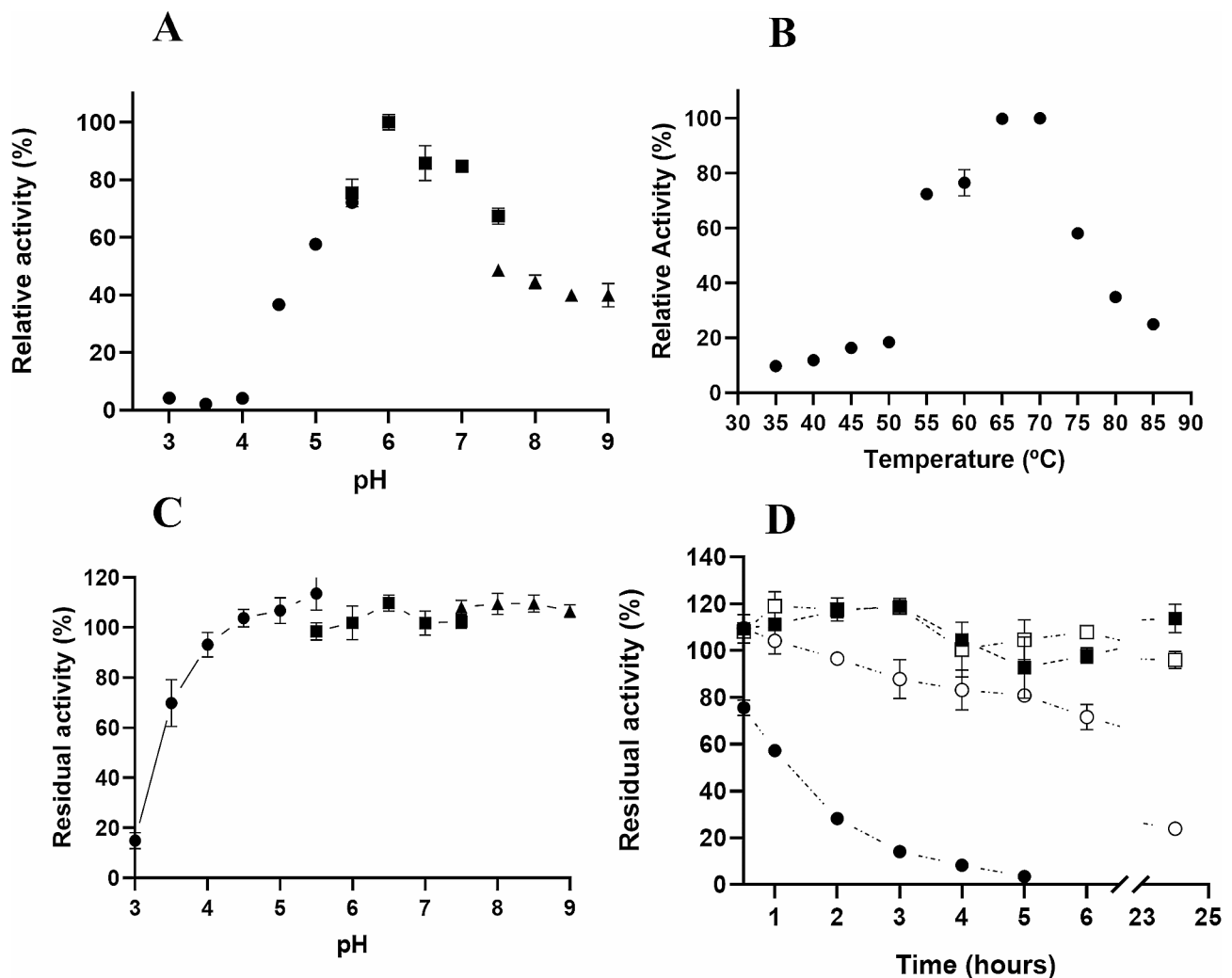


Fig. 4 Biochemical characterization of AnGH3. **(A)** Influence of optimum pH on enzymatic activity. Residual activities were assayed at 65 °C in the pH range of 3.0–5.5 with sodium citrate (●), pH 5.5–7.5 with sodium phosphate (■), and pH 7.5–9.0 with Tris–HCl buffers (▲). **(B)** Temperature influence on AnGH3. The purified enzyme was assayed at pH 6 in the 35–85 °C temperature range. **(C)** AnGH3 pH stability. The enzyme was incubated for 24 h, at 25 °C, at a pH range of 3.0 to 9.0. The residual activities were assayed at 65 °C and pH 6. The activity of the enzyme incubated in water was considered 100%. **(D)** Thermal denaturation of the purified AnGH3 at 45 °C (■), 50 °C (□), 55 °C (○) and 60 °C (●) up to 24 h. The residual activities concerning the initial enzyme activities were calculated. The residual activities were assayed at 65 °C and pH 6. The enzyme activity at incubation time zero was considered 100%

Table 1 Substrate specificity of AnGH3

Substrate	Concentration	Specific activity (U mg ⁻¹)
ρNPG	2 mmol L ⁻¹	282 ± 17
ρNPGal	2 mmol L ⁻¹	ND
ρNPX	2 mmol L ⁻¹	0.1 ± 0.01
α-ρNPG	2 mmol L ⁻¹	ND
ρNPCel	2 mmol L ⁻¹	4.5 ± 0.1
Cellobiose	1%	56 ± 0.3
CMC	1%	ND
Lactose	1%	ND
Salicin	1%	40 ± 0.8

ND, not detected

Substrate specificity of AnGH3

Various substrates were employed to explore the substrate specificity of AnGH3, and the findings are summarized in Table 1 and Fig. S2. The soluble enzyme demonstrated efficient hydrolysis of substrates featuring (1→4)-beta-glycosidic linkages, such as ρNPG, cellobiose, ρNPCel, and salicin. The most pronounced hydrolytic activity was observed with ρNPG (282 U mg⁻¹), followed by cellobiose disaccharide (56 U mg⁻¹), the glycoside of salicin (40 U mg⁻¹), and ρNPCel (4.5 U mg⁻¹). Additionally, the enzyme exhibited hydrolytic capability towards the glycoside of ρNPX but showed no activity against CMC, ρNPGal, and α-glycosidic bonds like α-ρNPG.

Several GH3 β -glucosidases capable of hydrolyzing not only ρ NPG and cellobiose but also other cello-oligosaccharides have been reported (Liu et al. 2012; Yan et al. 2012; Zhao et al. 2015; Ramani et al. 2015; Pei et al. 2016; Volkov et al. 2020; Dadwal et al. 2023). These enzymes display significant activity on diverse substrates and are often classified as broad-specificity β -glucosidases (Molina et al. 2016). The AnGH3 exhibited higher specificity activity for both ρ NPG and cellobiose compared to most family GH3 β -glucosidases, including MtBgl3b from *M. thermophila* (258 and 62 U mg⁻¹) (Zhao et al. 2015), nBgl3 from *A. fumigatus* (101 and 59 U mg⁻¹) (Liu et al. 2012), PtBglu3 from *Paecilomyces thermophila* (228 and 113 U mg⁻¹) (Yan et al. 2012), rAnBGL from *Penicillium verruculosum* (100 and 124 U mg⁻¹) (Volkov et al. 2020), MtBgl3c from *M. thermophila* (66 and 46 U mg⁻¹) (Dadwal et al. 2023), BGL2 from *N. crassa* (143 and 74 U mg⁻¹) (Pei et al. 2016).

According to Rajoka and colleagues (Rajoka et al. 2015), the variations in substrate specificity between ρ NPG and cellobiose arise from distinct interactions between various side chain residues of the β -glucosidase and each substrate. The authors performed structural analysis and docking studies with the thermostable β -glucosidase

from *Thermotoga maritima* using cellobiose and ρ NP-linked substrates. In the enzyme- ρ NPG complex, the interaction occurred via three hydrogen bonds with the active site residues Glu¹⁶⁶, Tyr²⁹⁵, and Asn²²³. In contrast, in the enzyme-cellobiose complex, the reaction involved residues Asn²²³, Ser²²⁹, and His²⁹⁸, forming hydrogen bonds with the ligand. Further structural investigations into these kinetic differences, particularly in fungi, are essential for future rational designs of β -glucosidases variants with improved properties.

Effect of biomass-derived compounds on AnGH3 activity

Various concentrations of xylose (0–2 mol L⁻¹) (Fig. 5A), ethanol (0–50% v/v) (Fig. 5B), glucose (0–1 mol L⁻¹) (Fig. 5C), furfural (0–200 mmol L⁻¹) and 5-HMF (0–200 mmol L⁻¹) (Fig. 5D) exhibited contrasting effects on AnGH3 activity. Surprisingly, AnGH3 activity was significantly stimulated by xylose (Fig. 5A), reaching a maximal 2.2-fold stimulation at 0.4 mol L⁻¹. Furthermore, the enzyme retained 100% activity even at high xylose concentrations of 1.5 mol L⁻¹. In contrast, in the presence of 25 mmol L⁻¹ and 200 mmol L⁻¹ of glucose (Fig. 5C), the relative enzymatic activity decreased by 53 and 10% relative to the control, respectively. Similar

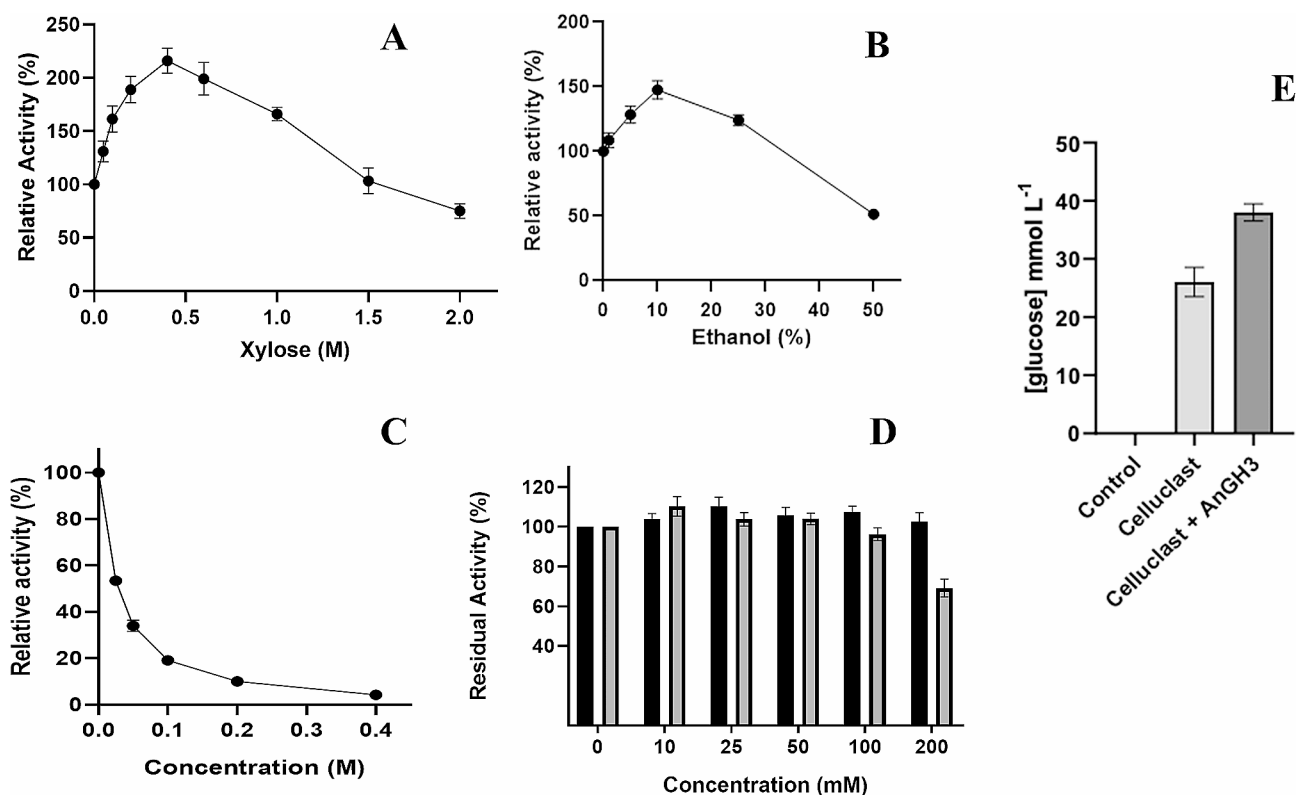


Fig. 5 Effect of different compounds on AnGH3 activity. **(A)** Xylose effect on the AnGH3 activity. **(B)** Ethanol effect on the AnGH3 activity. **(C)** Effect of glucose concentration in AnGH3 activity. **(D)** Furfural (black bar) and 5-HMF (gray bar) effect on AnGH3 activity. The purified enzyme was assayed at 65 °C pH 6; the activity without additive was considered 100%. The residual activities concerning the initial enzyme activities were calculated. **(E)** Cellulosic biomass hydrolysis for 24 h at 50 °C, pH 5.0 using AnGH3 and Celluclast® 1.5 L. All measurements were done in triplicates. Error bars show SD

results were reported for β -glucosidase from the thermophilic fungus *Humicola brevis* var. *thermoidea*. The enzyme showed a maximal increase of about 1.7-fold at 200 mmol L⁻¹ xylose and retained around 30% of its activity in the presence of 30 mmol L⁻¹ glucose (Masui et al. 2012). However, xylose-stimulated β -glucosidases are usually reported with concomitant glucose stimulation, as observed in the intracellular β -glucosidases of the thermophilic fungi *H. insolens* (Souza et al. 2010), *H. grisea* var. *thermoidea* (Nascimento et al. 2010), *Scytalidium thermophilum* (Zanoelo et al. 2004), and the thermophilic bacterium *Anoxybacillus flavithermus* subsp. *yunnensis* E13T (Liu et al. 2017). For these enzymes, studies suggest a regulatory binding site for glucose that is different from the active site, likely inducing conformational changes that stimulate the hydrolysis activity (Souza et al. 2013). GH3 β -glucosidases are uncommonly stimulated by glucose (and consequently xylose); on the other hand, in GH1 β -glucosidases, the glucose and xylose stimulation effects appear to be closely related. Briefly, in GH1, it has been proposed that glucose and xylose compete for the same binding site for stimulation since the addition of an equimolar mixture of the two monosaccharides does not increase the enzyme activity in a synergistic way (Corrêa et al. 2021). The mechanisms of xylose-only activation of β -glucosidase are unknown and require further investigation.

The effect of furfural and 5-HMF on enzyme activity was also tested (Fig. 5D). These lignocellulose pretreatment-derived compounds did not affect the enzymatic activity of AnGH3, even at concentrations up to 100 mmol L⁻¹. Additionally, the enzyme retained 100 and 70% of its activity in the presence of high concentrations (200 mmol L⁻¹) of furfural, and 5-HMF, respectively. These results surpassed those reported for β -glucosidase from *A. niger* URM 6642 (Oriente et al. 2015), commercial cellulase (Qi et al. 2018), and Lfa2 from metagenomic DNA isolated from soil samples (Alves et al. 2018). β -glucosidase from *A. niger* retained 86% of its activity in the presence of 40 mmol L⁻¹ furfural and 100% in the presence of 40 mmol L⁻¹ 5-HMF (Oriente et al. 2015). Similarly, the commercial cellulase (SunSon Group) displayed 100% of its initial activity in 5 g L⁻¹ (about 40

mmol L⁻¹) furfural (Qi et al. 2018). Lfa2 retained 70% of its activity in 10 g L⁻¹ (about 79 mmol L⁻¹) of furfural, and 100% in the presence of lower concentrations as 0.05 (about 4 mmol L⁻¹) and 0.1% (about 8 mmol L⁻¹), of 5-HMF. On the other hand, in 0.5 (about 40 mmol L⁻¹) and 1% (about 80 mmol L⁻¹), 5-HMF increased Lfa2 activity by 60 and 70%, respectively (Alves et al. 2018). Thus, although tolerance to lignocellulose-derived inhibitors like 5-HMF and furfural is crucial for the economic feasibility of enzymatic conversion of the lignocellulosic biomass, few studies test their effect on β -glucosidases.

The effect of ethanol on β -glucosidase activity is another fundamental analysis for its biotechnological application because the enzyme will be exposed to considerable ethanol concentrations, as in applications such as simultaneous saccharification, fermentation process, and winemaking (Su et al. 2022). β -glucosidase activity on ρ NPG was evaluated in the presence of ethanol at various concentrations (0–50%, v/v) (Fig. 5B). Surprisingly, enzyme activity was stimulated even at high concentrations of 25% ethanol. Furthermore, the enzyme maximized 1.5-fold stimulation in the presence of 10% ethanol. Literature has reported that changes in polarity in the reaction medium induced by alcohols could stabilize the conformation of the enzyme (Mateo and Di Stefano 1997; Karnaouri et al. 2013; El-Ghonemy 2021). Even at high concentrations of 50% ethanol, the enzyme retained 52% of its activity relative to the control, indicating that AnGH3 was highly ethanol tolerant. These results exceeded those reported for ethanol-tolerant β -glucosidase from *Aspergillus* sp. DHE7 (El-Ghonemy 2021), glucose tolerant GH3 β -glucosidase from *Malbranchea pulchella* (MpBgl3) (Monteiro et al. 2020), and GH3 β -glucosidases BglA, and BglJ from *A. oryzae* (Kudo et al. 2015). An improvement in the catalytic potential of some β -glucosidases in the presence of ethanol has been attributed to its glycosyl transferase activity (Wang et al. 2016; Mateo and Andreu 2020; El-Ghonemy 2021). In a reactional environment with high levels of alcohols compared to water levels, ethanol can act as an acceptor for the glycosyl moiety during catalysis of ρ NPG, resulting in higher reaction rates (Arévalo Villena et al. 2006; Wang et al. 2016; Mateo and Andreu 2020; El-Ghonemy 2021). However, at higher concentrations ($\geq 20\%$ v/v) of the polar solvents such as ethanol, the activity could be inhibited by conformational changes or denaturation (disruption of the secondary and tertiary structure) (Stepankova et al. 2013; Mateo 2023).

Kinetic parameters

Table 2 presents the kinetic parameters K_M , V_{max} , K_{cat} , and catalytic efficiency of the AnGH3 using ρ NPG and cellobiose as substrate. The recombinant enzyme showed higher specificity to ρ NPG than cellobiose, exhibiting

Table 2 The kinetic parameters of AnGH3 against ρ NPG and cellobiose hydrolysis at pH 6.0 and 65 °C

		V_{max} (U mg ⁻¹)	K_M (mmol L ⁻¹)	K_{cat} (s ⁻¹)	K_{cat}/K_M (mmol L ⁻¹ s ⁻¹)
ρ NPG	Michaelis-Menten	212	0.0607	275	4521
	Hanes-Woolf	211	0.0510	274	5371
cellobiose	Michaelis-Menten	56.7	2.71	73.5	27.2
	Hanes-Woolf	56	2.51	72.6	28.9

The values shown represent means \pm SD from triplicate assays ($n=3$)

K_M of 0.0607 mmol L⁻¹, V_{max} of 212 U mg⁻¹, and K_{cat} of 275 s⁻¹ under optimal conditions. The K_M and V_{max} of the AnGH3 using cellobiose were 2.7 mmol L⁻¹ and 57 U mg⁻¹, respectively.

Other GH3 produced in different expression systems show a wide range of kinetic parameter values (Table 3). However, AnGH3 showed a higher affinity for ρ NPG ($K_M = 0.0607$ mmol L⁻¹) compared to many other recombinant fungal β -glucosidases: BglA ($K_M = 0.75$ mmol L⁻¹) (Kudo et al. 2015), BglJ ($K_M = 0.48$ mmol L⁻¹) (Kudo et al. 2015), Cel3A ($K_M = 0.4$ mmol L⁻¹) (Gudmundsson et al. 2016), RmBglu3B ($K_M = 0.17$ mmol L⁻¹) (Guo et al. 2015). For cellobiose, the AnGH3 K_M value (2.7 mmol L⁻¹) was similar to the recombinant GH3 from *M. thermophila* ($K_M = 2.6$ mmol L⁻¹) (Karnaouri et al. 2013), rBgl3 from *A. fumigatus* Z5 ($K_M = 2.2$ mmol L⁻¹) (Liu et al. 2012), and commercial preparation Novozym 188 ($K_M = 2.4$ mmol L⁻¹) (Kao et al. 2019). In general, β -glucosidases show high catalytic activity and higher K_M with synthetic substrates (ρ NPG and methyl umbelliferyl β -D-glucoside (MUG)) compared to cellobiose. According to recent studies, the beta-glucosidase's kinetics depends on its substrate's configuration. These enzymes have a very rigid structure in the S1 substrate binding site, and one of the cellobiose glucose molecules needs to rotate to fit into the substrate binding site. This conformational change for catalysis is not required for ρ NPG because its small nitrophenyl group is relatively free to move in the S1 substrate binding site (Nam et al. 2010; Singhania et al. 2013; Bonfá et al. 2018).

In the present study, AnGH3 exhibited the apparent K_{cat} of 275 s⁻¹, using ρ NPG as the substrate. According to Cairns and Esen (Ketudat Cairns and Esen 2010), β -glucosidases usually have K_{cat} values of around 300 s⁻¹ or lower. In addition, AnGH3 showed a catalytic coefficient (K_{cat}/K_M) for ρ NPG of 4521 mmol L⁻¹ s⁻¹. Based on the literature values, this catalytic coefficient is one of the highest ever reported for β -glucosidase acting on this substrate (Erkanli et al. 2024), except for Bgl3A from *Talaromyces leycettanus* JCM12802 (Xia et al. 2016b). Other elevated K_{cat}/K_M values were reported to Bgl4 of *P. funiculosus* NCL1 ($K_{cat}/K_M = 2888$ mmol L⁻¹ s⁻¹) with ρ NPG, and ($K_{cat}/K_M = 3610$ mmol L⁻¹ s⁻¹) with cellobiose at 50 °C (Ramani et al. 2015); and BglA of *A. oryzae* ($K_{cat}/K_M = 868$ mmol L⁻¹ s⁻¹) using ρ NPG (Kudo et al. 2015).

Enzymatic saccharification of biomass

To investigate the potential application of the recombinant AnGH3 from *A. nidulans* in biomass conversion, the enzyme was combined with commercial extract Celluclast® 1.5 L using tropical forage grass (*P. maximum*) as the cellulosic material. The sample of tropical forage grass used had an estimated cellulose of 26.2±0.5%, hemicellulose of 20.5±0.2%, and an estimated total lignin of 26.3±0.8% (Freitas et al. 2021a). After 24 h hydrolysis at 50 °C, pH 5.0, the concentration of glucose released by Celluclast® 1.5 L alone was 25.6±0.4 mmol L⁻¹. When the hydrolysis using Celluclast® 1.5 L was combined with AnGH3, a 1.5-fold conversion (37.1±1.2 mmol

Table 3 General catalytic properties of AnGH3 compared with other GH3 β -Glucosidases

Source	Expression system	Substrate	Temperature/ pH optimum	V_{max} (U mg ⁻¹)	K_M (mmol L ⁻¹)	K_{cat} (s ⁻¹)	K_{cat}/K_M (mmol L ⁻¹ s ⁻¹)
<i>Aspergillus nidulans</i> (This work)	<i>A. nidulans</i>	ρ NPG	-	212	0.0607	275	4521
		cellobiose	65–70 °C / 6.0	56.7	2.71	73.5	27.2
<i>Aspergillus oryzae</i> (BglA) (Kudo et al. 2015)	<i>A. oryzae</i>	ρ NPG	50 °C / 5.5	456	0.75	651	868
<i>A. oryzae</i> (BglJ) (Kudo et al. 2015)	<i>A. oryzae</i>	ρ NPG	40 °C / 4.5	264	0.48	373	777
<i>Rasamsonia emersonii</i> (Gudmundsson et al. 2016)	<i>Hypocrea jecorina</i>	ρ NPG	37 °C / 5	-	0.40	5.4	13.5
		cellobiose	-	-	0.78	5.5	7.05
<i>Termitoga petrophila</i> (Xie et al. 2015)	<i>Escherichia coli</i>	ρ NPG	90 °C / 5	109	1.6	-	-
<i>Rhizomucor miehei</i> (Guo et al. 2015)	<i>E. coli</i>	ρ NPG	50 °C / 5	55.9	0.17	0.071	0.42
		cellobiose	-	33.5	3.7	0.043	0.012
<i>Humicola insolens</i> (Xia et al. 2016a)	<i>Pichia pastoris</i>	ρ NPG	60 °C / 5.5	46.2	0.90	73.1	81.6
		cellobiose	-	-	8.44	-	11.1
<i>Myceliophthora thermophila</i> (Karnaouri et al. 2013)	<i>P. pastoris</i>	ρ NPG	70 °C / 5	47.9	0.39	-	-
		cellobiose	-	49.4	2.64	-	-
<i>Chaetomella raphigera</i> (Kao et al. 2019)	<i>P. pastoris</i>	ρ NPG	70 °C / 5	419	0.2	-	-
		cellobiose	-	312	0.96	-	-
<i>Aspergillus fumigatus</i> Z5 (Liu et al. 2012)	<i>P. pastoris</i>	ρ NPG	60 °C / 6	131	1.76	-	-
		cellobiose	-	53	2.2	-	-
<i>Talaromyces leycettanus</i> (Xia et al. 2016b)	<i>P. pastoris</i>	ρ NPG	75 °C / 4.5	1309	0.18	1664	9096
		cellobiose	-	618	10.4	786	75.8

L⁻¹) increase was observed (Fig. 5E). Similar result was reported to recombinant β -glucosidase from *Thermoanaerobacterium aotearoense* when combined to commercial cellulase (Cellic[®] Ctec2) and applied in the sugarcane bagasse hydrolysis. The supplement of the purified β -glucosidase provided about 20% enhancement of the released reducing sugars (1.2-fold than of commercial cellulase alone) after a 70 h reaction at 50 °C pH 6.0 (Yang et al. 2015). Cao and coworkers (Cao et al. 2015) using β -glucosidase (Bgl6) isolated from a metagenomic library with the commercial cellulase (Celluclast[®] 1.5 L) to hydrolyze pretreated sugarcane bagasse resulted in about 1.5-fold more conversion (15% more conversion) than using Celluclast[®] 1.5 L alone after 240 h at 50 °C pH 6.0. This previous study demonstrated the high potential of AnGH3 to act in lignocellulosic biomass degradation cocktails. Thus, more studies are being carried out in our research group to optimize its application in biomass hydrolysis.

Conclusion

In this work, the gene *anGH3* encoding the β -glucosidase from *A. nidulans* FGSC A4 was functionally expressed and secreted by the homologous host strain *A. nidulans* A773. The purified β -glucosidase AnGH3 showed activity and stability at pH and temperature values similar to the conditions needed for biomass hydrolysis. In addition, AnGH3 was stimulated by D-xylose and ethanol molecules, was tolerant to phenolic compounds, and showed good kinetic properties. Thus, the biochemical assays demonstrated that the enzyme could be a promising candidate for industrial applications in enzymatic cocktails.

Furthermore, we believe these properties can be further improved by immobilizing the enzyme, increasing its operational performance and, therefore, the cost-benefit ratio of its lignocellulosic hydrolysis application. The appropriate choice of support, functional groups, and the strategy and protocol involved in immobilization can increase AnGH3 stability even more (more comprehensive pH, activity, temperature profiles, increased reuse cycles, etc.). In addition, the interaction of the enzyme with the support can cause conformational changes that can promote some positive effects on the enzyme's characteristics. For example, the immobilization of AnGH3 in the presence of its stimulating compounds, ethanol and xylose, can make it immobilized in the "hyperactivated" state or, in some instances, prevent inhibitions. That way, the potential of AnGH3 immobilization opens excellent possibilities to expand its peculiar characteristics (Di Cosimo et al. 2013; Sheldon and van Pelt 2013; Rodrigues et al. 2021; Bolivar et al. 2022).

Supplementary Information

The online version contains supplementary material available at <https://doi.org/10.1186/s40643-024-00784-2>.

Supplementary Material 1: Amino acid sequence of the β -glucosidase AnGH3 from *Aspergillus nidulans* FGSC A4. The peptides corresponding to those identified by mass spectrometry are underlined and in bold

Supplementary Material 2: Scheme of the different compounds used to measure the AnGH3 activity from *A. nidulans*. This manuscript also supports the "supplementary file" with a full uncropped Gel image

Supplementary Material 3

Acknowledgements

We thank Mauricio de Oliveira for their technical assistance.

Author contributions

Conceptualization, methodology, writing—review and editing: DA., RCA.; data curation, software, validation, formal analysis, investigation, review and editing, visualization: DA., RCA., PZA., JCSS., GSA., RJW., GLB., FS.; review, resources and funding acquisition: RCA., DA., JCSS., RJW., FS., MSB; writing—review and editing, resources, supervision, project administration, funding acquisition: MLTMP.

Funding

The authors gratefully acknowledge the São Paulo Research Foundation (FAPESP) (Grant n^o: 2018/07522-6, 2021/06679-1, 2022/00539-6, and 2023/01547-5; FCT (POCI-01-0145-FEDER-032206)—transnational cooperation project EcoTech, Conselho Nacional de Desenvolvimento Científico e Tecnológico (CNPq) (310340/2021-7), and National Institute of Science and Technology of Bioethanol (INCT) (CNPq 465319/2014-9/FAPESP n^o 2014/50884-5) for financial support. Research scholarships were granted to RCA by CNPq (Grant n^o: 151187/2023-1) and by FAPESP (Grant n^o: 2023/09627-8); to DA by FAPESP (Grant n^o: 2020/15510-8 and 2023/01338-7); to JCSS by CNPq (Grant n^o: 384465/2023-4) and FAPESP (Grant n^o: 2019/21989-7), and GSA by CAPES (Coordenação de Aperfeiçoamento de Pessoal de Nível Superior, Finance Code 001).

Data availability

The datasets used and/or analyzed during the current study are available from the corresponding author upon reasonable request.

Declarations

Ethics approval and consent to participate

This article contains no studies performed by authors with human participants or animals.

Consent for publication

All authors approved the consent for publishing the manuscript to *Bioresources and Bioprocessing*.

Competing interests

The authors declare that they have no competing interests.

Author details

¹Department of Biology, Faculty of Philosophy, Sciences and Letters of Ribeirão Preto, University of São Paulo, Ribeirão Preto, SP 14040-901, Brazil

²Department of Biochemistry and Immunology, Faculty of Medicine of Ribeirão Preto, University of São Paulo, Ribeirão Preto, SP 14049-900, Brazil

³Laboratory of Enzymology and Molecular Biology of Microorganisms, Institute of Biology, Campinas State University (UNICAMP), Campinas 13083-970, SP, Brazil

⁴Department of Chemistry, Faculty of Philosophy, Sciences and Letters of Ribeirão Preto, University of São Paulo, Ribeirão Preto, SP 14040-901, Brazil

⁵Department of Biotechnology, Lorena School of Engineering, University of São Paulo, Lorena 12602-810, Brazil

⁶Bioscience Institute, University of São Paulo, São Paulo 05508-090, Brazil

Received: 1 April 2024 / Accepted: 3 July 2024

Published online: 29 July 2024

References

- Acharya S, Liyanage S, Parajuli P et al (2021) Utilization of cellulose to its full potential: a review on Cellulose Dissolution, Regeneration, and applications. *Polym (Basel)* 13. <https://doi.org/10.3390/polym13244344>
- Agrawal R, Semwal S, Kumar R et al (2018) Synergistic enzyme cocktail to enhance hydrolysis of steam exploded wheat straw at pilot scale. *Frontiers in Energy Research* 6:122. <https://doi.org/10.3389/fenrg.2018.00122>
- Ali N, Xue Y, Gan L et al (2016) Purification, characterization, gene cloning and sequencing of a new β -glucosidase from *Aspergillus niger* BE-2. *Appl Biochem Microbiol* 52:564–571. <https://doi.org/10.1134/S0003683816050045>
- Alnoch RC, Alves GS, Salgado JCS et al (2022) Immobilization and application of the recombinant xylanase GH10 of *Malbranchea pulchella* in the production of xylooligosaccharides from hydrothermal liquor of the eucalyptus (*Eucalyptus grandis*) Wood chips. *Int J Mol Sci* 23, 13329. <https://doi.org/10.3390/ijms232113329>
- Alnoch RC, Salgado JCS, Alves GS et al (2023) Biochemical characterization of an endoglucanase GH7 from Thermophile *Thermothielavioides terrestris* expressed on *Aspergillus nidulans*. *Catalysts* 13. <https://doi.org/10.3390/catal13030582>
- Alves L, de Meleiro F, Silva LP RN, et al (2018) Novel ethanol- and 5-Hydroxymethyl furfural-stimulated β -Glucosidase retrieved from a Brazilian secondary atlantic forest soil metagenome. *Front. Microbiol.* 9:2556. <https://doi.org/10.3389/fmicb.2018.02556>
- Arévalo Villena M, Úbeda Iranzo JF, Gundllapalli SB et al (2006) Characterization of an exocellular β -glucosidase from *Debaryomyces pseudopolymorphus*. *Enzyme Microb Technol* 39:229–234. <https://doi.org/10.1016/j.enzmictec.2005.10.018>
- Bajpai P (2018) Chap. 9 - paper Bioprocessing. In: Third E (ed) Bajpai PBT-BH of P and P. Elsevier, pp 187–205
- Berman HM, Westbrook J, Feng Z et al (2000) The Protein Data Bank. *Nucleic Acids Res* 28:235–242. <https://doi.org/10.1093/nar/28.1.235>
- Bolivar JM, Woodley JM, Fernandez-Lafuente R (2022) Is enzyme immobilization a mature discipline? Some critical considerations to capitalize on the benefits of immobilization. *Chem Soc Rev* 51:6251–6290. <https://doi.org/10.1039/d2cs00083k>
- Bonfá EC, de Souza Moretti MM, Gomes E, Bonilla-Rodríguez GO (2018) Biochemical characterization of an isolated 50 kDa beta-glucosidase from the thermophilic fungus *Myceliophthora thermophila* M.7.7. *Biocatal Agric Biotechnol* 13:311–318. <https://doi.org/10.1016/j.bcab.2018.01.008>
- Bradford MM (1976) A rapid and sensitive method for the quantitation of microgram quantities of protein utilizing the principle of protein-dye binding. *Anal Biochem* 72:248–254. [https://doi.org/10.1016/0003-2697\(76\)90527-3](https://doi.org/10.1016/0003-2697(76)90527-3)
- Brigham C (2018) In: Török B, Dransfield TBT-GC (eds) Chap. 3.22 - biopolymers: Biodegradable Alternatives to Traditional Plastics. Elsevier, pp 753–770
- Cao L-C, Wang Z-J, Ren G-H, et al (2015) Engineering a novel glucose-tolerant β -glucosidase as supplementation to enhance the hydrolysis of sugarcane bagasse at high glucose concentration. *Biotechnol Biofuels*. <https://doi.org/10.1186/s13068-015-0383-z>
- Chalkley RJ, Baker PR, Hansen KC et al (2005) Comprehensive analysis of a multidimensional liquid chromatography mass spectrometry dataset acquired on a quadrupole selecting, quadrupole collision cell, time-of-flight mass spectrometer: I. how much of the data is theoretically interpretable by search. *Mol Cell Proteom* 4:1189–1193. <https://doi.org/10.1074/mcp.D500001-MCP200>
- Chang F, Xue S, Xie X et al (2018) Carbohydrate-binding module assisted purification and immobilization of β -glucosidase onto cellulose and application in hydrolysis of soybean isoflavone glycosides. *J Biosci Bioeng* 125:185–191. <https://doi.org/10.1016/j.jbiosc.2017.09.001>
- Corrêa TLR, Franco Cairo JPL, Cota J et al (2021) A novel mechanism of β -glucosidase stimulation through a monosaccharide binding-induced conformational change. *Int J Biol Macromol* 166:1188–1196. <https://doi.org/10.1016/j.jbiomac.2020.11.001>
- Dadwal A, Sharma S, Satyanarayana T (2023) Biochemical characteristics of *Myceliophthora thermophila* recombinant β -glucosidase (MtBgl3c) applicable in cellulose bioconversion. *Prep Biochem Biotechnol* 1–12. <https://doi.org/10.1016/10826068.2023.2177869>
- Daly P, van Munster JM, Blythe MJ et al (2017) Expression of *Aspergillus niger* CAZymes is determined by compositional changes in wheat straw generated by hydrothermal or ionic liquid pretreatments. *Biotechnol Biofuels* 10:35. <https://doi.org/10.1186/s13068-017-0700-9>
- de Andrades D, Graebin NG, Kadowaki MK et al (2019a) Immobilization and stabilization of different β -glucosidases using the glutaraldehyde chemistry: optimal protocol depends on the enzyme. *Int J Biol Macromol* 129:672–678. <https://doi.org/10.1016/j.jbiomac.2019.02.057>
- de Andrades D, Graebin NG, Ayub MAZ et al (2019b) Physico-chemical properties, kinetic parameters, and glucose inhibition of several beta-glucosidases for industrial applications. *Process Biochem* 78:82–90. <https://doi.org/10.1016/j.procbio.2019.01.008>
- de Freitas EN, Alnoch RC, Contato AG et al (2021a) Enzymatic pretreatment with Laccases from *Lentinus sajor-caju* induces structural modification in Lignin and enhances the digestibility of Tropical Forage Grass (*Panicum maximum*) grown under future climate conditions. *Int J Mol Sci* 22. <https://doi.org/10.3390/ijms22179445>
- de Freitas EN, Salgado JCS, Alnoch RC et al (2021b) Challenges of Biomass Utilization for Bioenergy in a Climate Change Scenario. *Biology (Basel)* 10. <https://doi.org/10.3390/biology10121277>
- Di Cosimo R, Mc Auliffe J, Poulouse AJ, Bohlmann G (2013) Industrial use of immobilized enzymes. *Chem Soc Rev* 42:6437–6474. <https://doi.org/10.1039/c3cs35506c>
- El-Ghonemy DH (2021) Optimization of extracellular ethanol-tolerant β -glucosidase production from a newly isolated *Aspergillus* sp. DHE7 via solid state fermentation using jojoba meal as substrate: purification and biochemical characterization for biofuel preparation. *J Genetic Eng Biotechnol* 19:45. <https://doi.org/10.1186/s43141-021-00144-z>
- Erkanli ME, El-Halabi K, Kim JR (2024) Exploring the diversity of β -glucosidase: classification, catalytic mechanism, molecular characteristics, kinetic models, and applications. *Enzyme Microb Technol* 173:110363. <https://doi.org/10.1016/j.enzmictec.2023.110363>
- Etale A, Onyianta AJ, Turner SR, Eichhorn SJ (2023) Cellulose: a review of water interactions, applications in composites, and Water Treatment. *Chem Rev* 123:2016–2048. <https://doi.org/10.1021/acs.chemrev.2c00477>
- Fleissner A, Dersch P (2010) Expression and export: recombinant protein production systems for *Aspergillus*. *Appl Microbiol Biotechnol* 87:1255–1270. <https://doi.org/10.1007/s00253-010-2672-6>
- Fusco FA, Fiorentino G, Pedone E et al (2018) Biochemical characterization of a novel thermostable β -glucosidase from *Dictyoglomus turgidum*. *Int J Biol Macromol* 113:783–791. <https://doi.org/10.1016/j.jbiomac.2018.03.018>
- Gibson DG, Young L, Chuang R-Y et al (2009) Enzymatic assembly of DNA molecules up to several hundred kilobases. *Nat Methods* 6:343–345. <https://doi.org/10.1038/nmeth.1318>
- Gonçalves AL, Cunha PM, da Silva Lima A et al (2023) Production of recombinant lytic polysaccharide monoxygenases and evaluation effect of its addition into *Aspergillus fumigatus* var. *niveus* cocktail for sugarcane bagasse saccharification. *Biochim Biophys Acta (BBA) - Proteins Proteom* 1871:140919. <https://doi.org/10.1016/j.bbapap.2023.140919>
- Gudmundsson M, Hansson H, Karkehabadi S et al (2016) Structural and functional studies of the glycoside hydrolase family 3 β -glucosidase Cel3A from the moderately thermophilic fungus *Rasamsonia emersonii*. *Acta Crystallogr D Struct Biol* 72:860–870. <https://doi.org/10.1107/S2059798316008482>
- Guo Y, Yan Q, Yang Y et al (2015) Expression and characterization of a novel β -glucosidase, with transglycosylation and exo- β -1,3-glucanase activities, from *Rhizomucor miehei*. *Food Chem* 175:431–438. <https://doi.org/10.1016/j.foodchem.2014.12.004>
- Gupta R, Brunak S (2002) Prediction of glycosylation across the human proteome and the correlation to protein function. *Pac Symp Biocomput* 310–322, PMID: 11928486.
- Hanes CS (1932) Studies on plant amylases: the effect of starch concentration upon the velocity of hydrolysis by the amylase of germinated barley. *Biochem J* 26:1406–1421. <https://doi.org/10.1042/bj0261406>
- Hildén K, Mäkelä, MRBT-RM in LS (2018) Role of Fungi in Wood Decay. Elsevier
- Huang C, Feng Y, Patel G et al (2021) Production, immobilization and characterization of beta-glucosidase for application in cellulose degradation from a novel *Aspergillus versicolor*. *Int J Biol Macromol* 177:437–446. <https://doi.org/10.1016/j.jbiomac.2021.02.154>
- Isikgor FH, Becer CR (2015) Lignocellulosic biomass: a sustainable platform for the production of bio-based chemicals and polymers. *Polym Chem* 6:4497–4559. <https://doi.org/10.1039/c5py00263j>
- Jumper J, Evans R, Pritzel A et al (2021) Highly accurate protein structure prediction with AlphaFold. *Nature* 596:583–589. <https://doi.org/10.1038/s41586-021-03819-2>

- Kao M-R, Kuo H-W, Lee C-C et al (2019) *Chaetomella raphigera* β -glucosidase D2-BGL has intriguing structural features and a high substrate affinity that renders it an efficient cellulase supplement for lignocellulosic biomass hydrolysis. *Biotechnol Biofuels* 12:258. <https://doi.org/10.1186/s13068-019-1599-0>
- Karkehabadi S, Helmich KE, Kaper T et al (2014) Biochemical characterization and Crystal Structures of a Fungal Family 3 β -Glucosidase, Cel3A from *Hypocrea jecorina*. *J Biol Chem* 289:31624–31637. <https://doi.org/10.1074/jbc.M114.587766>
- Karnaouri A, Topakas E, Paschos T et al (2013) Cloning, expression and characterization of an ethanol tolerant GH3 β -glucosidase from *Myceliophthora thermophila*. *PeerJ* 1:e46. <https://doi.org/10.7717/peerj.46>
- Ketudat Cairns JR, Esen A (2010) β -Glucosidases. *Cell Mol Life Sci* 67:3389–3405. <https://doi.org/10.1007/s00018-010-0399-2>
- Kück U, Hoff B (2010) New tools for the genetic manipulation of filamentous fungi. *Appl Microbiol Biotechnol* 86:51–62. <https://doi.org/10.1007/s00253-009-2416-7>
- Kudo K, Watanabe A, Ujiiie S et al (2015) Purification and enzymatic characterization of secretory glycoside hydrolase family 3 (GH3) aryl β -glucosidases screened from *Aspergillus oryzae* genome. *J Biosci Bioeng* 120:614–623. <https://doi.org/10.1016/j.jbiosc.2015.03.019>
- Laemmli UK (1970) Cleavage of structural proteins during the Assembly of the Head of Bacteriophage T4. *Nature* 227:680–685. <https://doi.org/10.1038/227680a0>
- Lima RAT, De Oliveira G, Souza AA et al (2020) Functional and structural characterization of a novel GH3 β -glucosidase from the gut metagenome of the Brazilian Cerrado termite *Syntermes wheeleri*. *Int J Biol Macromol* 165:822–834. <https://doi.org/10.1016/j.jbiomac.2020.09.236>
- Liu D, Zhang R, Yang X et al (2012) Characterization of a thermostable β -glucosidase from *Aspergillus fumigatus* Z5, and its functional expression in *Pichia pastoris* X33. *Microb Cell Fact* 11:25. <https://doi.org/10.1186/1475-2859-11-25>
- Liu Y, Li R, Wang J et al (2017) Increased enzymatic hydrolysis of sugarcane bagasse by a novel glucose- and xylose-stimulated β -glucosidase from *Anoxybacillus flavithermus* subsp. *yunnanensis* E13T. *BMC Biochem* 18:4. <https://doi.org/10.1186/s12858-017-0079-z>
- Liu E, Segato F, Wilkins MR (2021) Fed-batch production of *Thermothelomyces thermophilus* lignin peroxidase using a recombinant *Aspergillus nidulans* strain in stirred-tank bioreactor. *Bioresour Technol* 325:124700. <https://doi.org/10.1016/j.biortech.2021.124700>
- Lubertozzi D, Keasling JD (2009) Developing *Aspergillus* as a host for heterologous expression. *Biotechnol Adv* 27:53–75. <https://doi.org/10.1016/j.biotechadv.2008.09.001>
- Masui DC, Zimbardi ALRL, Souza FHM et al (2012) Production of a xylose-stimulated β -glucosidase and a cellulase-free thermostable xylanase by the thermophilic fungus *Humicola brevis* var. *thermoidea* under solid state fermentation. *World J Microbiol Biotechnol* 28:2689–2701. <https://doi.org/10.1007/s11274-012-1079-1>
- Mateo JJ (2023) Physico-Chemical characterization of an exocellular sugars tolerant β -glucosidase from grape *Metschnikowia pulcherrima* isolates. *Microorganisms* 11. <https://doi.org/10.3390/microorganisms11040964>
- Mateo JJ, Andreu L (2020) Characterization of an exocellular ethanol-tolerant β -glucosidase from *Quambalaria cyanescens* isolates from unripened grapes. *Eur Food Res Technol* 246:2349–2357. <https://doi.org/10.1007/s00217-020-03578-w>
- Mateo JJ, Di Stefano R (1997) Description of the β -glucosidase activity of wine yeasts. *Food Microbiol* 14:583–591. <https://doi.org/10.1006/fmic.1997.0122>
- McKendry P (2002) Energy production from biomass (part 1): overview of biomass. *Bioresour Technol* 83:37–46. [https://doi.org/10.1016/S0960-8524\(01\)00118-3](https://doi.org/10.1016/S0960-8524(01)00118-3)
- Méndez-Liter JA, Gil-Muñoz J, Nieto-Domínguez M et al (2017) A novel, highly efficient β -glucosidase with a cellulose-binding domain: characterization and properties of native and recombinant proteins. *Biotechnol Biofuels* 10:256. <https://doi.org/10.1186/s13068-017-0946-2>
- Michelin M, Gomes DG, Romani A et al (2020) Nanocellulose production: exploring the enzymatic route and residues of pulp and paper industry. *Molecules* 25, 3411. <https://doi.org/10.3390/molecules25153411>
- Miles AJ, Ramalli SG, Wallace BA (2022) DichroWeb, a website for calculating protein secondary structure from circular dichroism spectroscopic data. *Protein Sci* 31:37–46. <https://doi.org/10.1002/pro.4153>
- Miller GL (1959) Use of Dinitrosalicylic Acid Reagent for determination of reducing Sugar. *Anal Chem* 31:426–428. <https://doi.org/10.1021/ac60147a030>
- Mishra S, Goyal D, Kumar A, Dantu PK (2019) Biotechnological applications of β -Glucosidases in Biomass Degradation. In: Yadav AN, Singh S, Mishra S, Gupta A (eds) Recent Advancement in White Biotechnology through Fungi. *Fungal Biology*. Springer International Publishing, Cham, pp 257–281
- Molina G, Contesini FJ, de Melo RR et al (2016) Chap. 11 - β -Glucosidase from *Aspergillus* In: Gupta VKBT-N and FD in MB and B (ed). Elsevier, Amsterdam, pp 155–169
- Monteiro LMO, Vici AC, Pinheiro MP et al (2020) A highly glucose tolerant β -Glucosidase from *Malbranchea pulchella* (MpBg3) enables cellulose saccharification. *Sci Rep* 10:6998. <https://doi.org/10.1038/s41598-020-63972-y>
- Mussatto SI, Yamakawa CK, van der Maas L, Dragone G (2021) New trends in bioprocesses for lignocellulosic biomass and CO₂ utilization. *Renew Sustain Energy Rev* 152:111620. <https://doi.org/10.1016/j.rser.2021.111620>
- Nam KH, Sung MW, Hwang KY (2010) Structural insights into the substrate recognition properties of β -glucosidase. *Biochem Biophys Res Commun* 391:1131–1135. <https://doi.org/10.1016/j.bbrc.2009.12.038>
- Nascimento CV, Souza FHM, Masui DC et al (2010) Purification and biochemical properties of a glucose-stimulated β -D-glucosidase produced by *Humicola grisea* var. *thermoidea* grown on sugarcane bagasse. *J Microbiol* 48:53–62. <https://doi.org/10.1007/s12275-009-0159-x>
- Oriente A, Tramontina R, de Andrades D et al (2015) Characterization of a novel *Aspergillus niger* beta-glucosidase tolerant to saccharification of lignocellulosic biomass products and fermentation inhibitors. *Chem Pap* 69:1050–1057. <https://doi.org/10.1515/chempap-2015-0111>
- Ouyang B, Wang G, Zhang N et al (2023) Recent advances in β -Glucosidase sequence and structure Engineering: a brief review. *Molecules* 28. <https://doi.org/10.3390/molecules28134990>
- Pei X, Zhao J, Cai P et al (2016) Heterologous expression of a GH3 β -glucosidase from *Neurospora crassa* in *Pichia pastoris* with high purity and its application in the hydrolysis of soybean isoflavone glycosides. *Protein Expr Purif* 119:75–84. <https://doi.org/10.1016/j.pep.2015.11.010>
- Perkins DN, Pappin DJC, Creasy DM, Cottrell JS (1999) Probability-based protein identification by searching sequence databases using mass spectrometry data. *Electrophoresis* 20:3551–3567. [https://doi.org/10.1002/\(SICI\)1522-2683\(19991201\)20:18%3C3551::AID-ELPS3551%3E3.0.CO;2-2](https://doi.org/10.1002/(SICI)1522-2683(19991201)20:18%3C3551::AID-ELPS3551%3E3.0.CO;2-2)
- Pettersen EF, Goddard TD, Huang CC et al (2021) UCSF ChimeraX: structure visualization for researchers, educators, and developers. *Protein Sci* 30:70–82. <https://doi.org/10.1002/pro.3943>
- Qi B, Luo J, Wan Y (2018) Immobilization of cellulase on a core-shell structured metal-organic framework composites: better inhibitors tolerance and easier recycling. *Bioresour Technol* 268:577–582. <https://doi.org/10.1016/j.biortech.2018.07.115>
- Rajoka MI, Idrees S, Ashfaq UA et al (2015) Determination of substrate specificities against β -Glucosidase A (BglA) from *Thermotoga maritima*: a Molecular Docking Approach. *J Microbiol Biotechnol* 25:44–49. <https://doi.org/10.4014/jmb.1312.12043>
- Ramani G, Meera B, Vanitha C et al (2015) Molecular cloning and expression of the thermostable glucose-tolerant β -glucosidase of *Penicillium funiculosum* NCL1 in *Pichia pastoris* and its characterization. *J Ind Microbiol Biotechnol* 42:553–565. <https://doi.org/10.1007/s10295-014-1549-6>
- Ribeiro LFC, De Lucas RC, Vitcosque GL et al (2014) A novel thermostable xylanase GH10 from *Malbranchea pulchella* expressed in *Aspergillus nidulans* with potential applications in biotechnology. *Biotechnol Biofuels* 7:115. <https://doi.org/10.1186/1754-6834-7-115>
- Robert X, Gouet P (2014) Deciphering key features in protein structures with the new ENDscript server. *Nucleic Acids Res* 42:W320–W324. <https://doi.org/10.1093/nar/gku316>
- Rodrigues RC, Berenguer-Murcia Á, Carballeas D et al (2021) Stabilization of enzymes via immobilization: multipoint covalent attachment and other stabilization strategies. *Biotechnol Adv* 52. <https://doi.org/10.1016/j.biotechadv.2021.107821>
- Salgado JCS, Meleiro LP, Carli S, Ward RJ (2018) Glucose tolerant and glucose stimulated β -glucosidases – a review. *Bioresour Technol* 267:704–713. <https://doi.org/10.1016/j.biortech.2018.07.137>
- Segato F, Damásio ARL, Gonçalves TA et al (2012) High-yield secretion of multiple client proteins in *Aspergillus*. *Enzyme Microb Technol* 51:100–106. <https://doi.org/10.1016/j.enzmictec.2012.04.008>
- Sharma S, Vaid S, Bhat B et al (2019) Chap. 17 - thermostable enzymes for Industrial Biotechnology. In: Singh RS, Singhania RR, Pandey A, Larroche CBT-A in ET (eds) *Biomass, Biofuels, Biochemicals*. Elsevier, pp 469–495
- Sheldon RA, van Pelt S (2013) Enzyme immobilisation in biocatalysis: why, what and how. *Chem Soc Rev* 42:6223–6235. <https://doi.org/10.1039/C3CS60075K>
- Singhania RR, Sukumaran RK, Rajasree KP et al (2011) Properties of a major β -glucosidase-BGL1 from *Aspergillus niger* NII-08121 expressed differentially

- in response to carbon sources. *Process Biochem* 46:1521–1524. <https://doi.org/10.1016/j.procbio.2011.04.006>
- Singhania RR, Patel AK, Sukumaran RK et al (2013) Role and significance of beta-glucosidases in the hydrolysis of cellulose for bioethanol production. *Bioreour Technol* 127:500–507. <https://doi.org/10.1016/j.biortech.2012.09.012>
- Solhtalab M, Flannelly DF, Aristilde L (2019) Substrate binding versus escape dynamics in a pH-affected fungal beta-glucosidase revealed by molecular dynamics simulations. *Carbohydr Res* 472:127–131. <https://doi.org/10.1016/j.carres.2018.12.007>
- Souza FHM, Nascimento CV, Rosa JC et al (2010) Purification and biochemical characterization of a mycelial glucose- and xylose-stimulated β -glucosidase from the thermophilic fungus *Humicola insolens*. *Process Biochem* 45:272–278. <https://doi.org/10.1016/j.procbio.2009.09.018>
- Souza FHM, Inocentes RF, Ward RJ et al (2013) Glucose and xylose stimulation of a β -glucosidase from the thermophilic fungus *Humicola insolens*: a kinetic and biophysical study. *J Mol Catal B: Enz* 94. <https://doi.org/10.1016/j.molcatb.2013.05.012>
- Srivastava N, Rathour R, Jha S et al (2019) Microbial Beta glucosidase enzymes: recent advances in Biomass Conversion for Biofuels Application. *Biomolecules* 9:220. <https://doi.org/10.3390/biom9060220>
- Stepankova V, Damborsky J, Chaloupkova R (2013) Organic co-solvents affect activity, stability and enantioselectivity of haloalkane dehalogenases. *Biotechnol J* 8:719–729. <https://doi.org/10.1002/biot.201200378>
- Su H, Xiao Z, Yu K et al (2022) Use of a purified β -glucosidase from coral-associated microorganisms to enhance wine aroma. *J Sci Food Agric* 102:3467–3474. <https://doi.org/10.1002/jsfa.11694>
- Sun S, Sun S, Cao X, Sun R (2016) The role of pretreatment in improving the enzymatic hydrolysis of lignocellulosic materials. *Bioreour Technol* 199:49–58. <https://doi.org/10.1016/j.biortech.2015.08.061>
- Thompson JD, Higgins DG, Gibson TJ (1994) CLUSTAL W: improving the sensitivity of progressive multiple sequence alignment through sequence weighting, position-specific gap penalties and weight matrix choice. *Nucleic Acids Res* 22:4673–4680. <https://doi.org/10.1093/nar/22.22.4673>
- Turner P, Mamo G, Karlsson EN (2007) Potential and utilization of thermophiles and thermostable enzymes in biorefining. *Microb Cell Fact* 6:9. <https://doi.org/10.1186/1475-2859-6-9>
- Velasco J, Oliva B, Gonçalves AL et al (2020) Functional characterization of a novel thermophilic exo-arabinanase from *Thermothielavioides terrestris*. *Appl Microbiol Biotechnol* 104:8309–8326. <https://doi.org/10.1007/s00253-020-10806-6>
- Volkov PV, Rozhkova AM, Zorov IN, Sinitsyn AP (2020) Cloning, purification and study of recombinant GH3 family β -glucosidase from *Penicillium verruculosum*. *Biochimie* 168:231–240. <https://doi.org/10.1016/j.biochi.2019.11.009>
- Wang X, Liu ZL, Weber SA, Zhang X (2016) Two new native β -Glucosidases from *Clavispora NRRL Y-50464* Confer its dual function as Cellobiose Fermenting Ethanologenic yeast. *PLoS ONE* 11:e0151293
- Ward OP (2012) Production of recombinant proteins by filamentous fungi. *Biotechnol Adv* 30:1119–1139. <https://doi.org/10.1016/j.biotechadv.2011.09.012>
- Wilson N, Simpson R, Cooper-Liddell C (2009) Introductory glycosylation analysis using SDS-PAGE and peptide Mass Fingerprinting. In: Packer NH, Karlsson NG (eds) *Glycomics: methods and protocols*. Humana, Totowa, NJ, pp 205–212
- Wojtusik M, Villar JC, Zurita M et al (2017) Study of the enzymatic activity inhibition on the saccharification of acid pretreated corn stover. *Biomass Bioenergy* 98:1–7. <https://doi.org/10.1016/j.biombioe.2017.01.010>
- Xia W, Bai Y, Cui Y et al (2016a) Functional diversity of family 3 β -glucosidases from thermophilic cellulolytic fungus *Humicola insolens* Y1. *Sci Rep* 6:27062. <https://doi.org/10.1038/srep27062>
- Xia W, Xu X, Qian L et al (2016b) Engineering a highly active thermophilic β -glucosidase to enhance its pH stability and saccharification performance. *Biotechnol Biofuels* 9:147. <https://doi.org/10.1186/s13068-016-0560-8>
- Xie J, Zhao D, Zhao L et al (2015) Overexpression and characterization of a Ca^{2+} activated thermostable β -glucosidase with high ginsenoside Rb1 to ginsenoside 20(S)-Rg3 bioconversion productivity. *J Ind Microbiol Biotechnol* 42:839–850. <https://doi.org/10.1007/s10295-015-1608-7>
- Yan Q, Hua C, Yang S et al (2012) High level expression of extracellular secretion of a β -glucosidase gene (PtBglu3) from *Paecilomyces thermophila* in *Pichia pastoris*. *Protein Expr Purif* 84:64–72. <https://doi.org/10.1016/j.pep.2012.04.016>
- Yan Q, Han L, Liu Z et al (2023) Stepwise genetic modification for efficient expression of heterologous proteins in *Aspergillus nidulans*. *Appl Microbiol Biotechnol* 107:6923–6935. <https://doi.org/10.1007/s00253-023-12755-2>
- Yang F, Yang X, Li Z et al (2015) Overexpression and characterization of a glucose-tolerant β -glucosidase from *T. aotearoense* with high specific activity for cellobiose. *Appl Microbiol Biotechnol* 99:8903–8915. <https://doi.org/10.1007/s00253-015-6619-9>
- Zanoelo FF, Polizeli MLTM, Terenzi HF, Jorge JA (2004) β -glucosidase activity from the thermophilic fungus *Scytalidium thermophilum* is stimulated by glucose and xylose. *FEMS Microbiol Lett* 240. <https://doi.org/10.1016/j.femsle.2004.09.021>
- Zhao J, Guo C, Tian C, Ma Y (2015) Heterologous expression and characterization of a GH3 β -Glucosidase from Thermophilic Fungi *Myceliophthora thermophila* in *Pichia pastoris*. *Appl Biochem Biotechnol* 177:511–527. <https://doi.org/10.1007/s12010-015-1759-z>
- Zoghalmi A, Paës G (2019) Lignocellulosic biomass: understanding recalcitrance and predicting hydrolysis. *Front Chem* 7:874. <https://doi.org/10.3389/fchem.2019.00874>

Publisher's Note

Springer Nature remains neutral with regard to jurisdictional claims in published maps and institutional affiliations.